

Earth's Magnetic Field: A New Look

The solar wind confines the geomagnetic field to form the magnetosphere and magnetic tail.

Norman F. Ness

Man's early view of the Earth's magnetic field began with the experimental work of men such as Robert Norman, a ship's instrument maker in London. It culminated in the publication in 1600 of William Gilbert's great treatise *De Magnete*. These individuals were interested in explaining a phenomenon which was first known by the ancients from the curious attractive properties of a lodestone. Used in a directional compass, these properties provided a means of navigation for commercial and exploratory endeavors. Although Gilbert's early theory of the origin of the geomagnetic field has not proved correct, his general conclusions on its geometry and character were amazingly accurate. Subsequent advances in the theoretical description of terrestrial magnetism came through the work of the mathematicians Laplace, Poisson, and finally Gauss, who in 1838 published a discussion of the mathematical analysis of the geomagnetic field. His application of potential theory and his development of spherical harmonic analysis form the cornerstones of modern techniques for studying the field.

The author is on the staff of the Laboratory for Space Sciences, Goddard Space Flight Center, National Aeronautics and Space Administration, Greenbelt, Maryland. This article was originally an address presented at the special session "Moving Frontiers in Science" of the AAAS meeting, Berkeley, California, 26 December 1965.

While its general spatial properties were being observed, characteristic temporal variations of the geomagnetic field were also identified. In 1806 von Humboldt deduced that there were periods, associated with auroral displays, during which the entire terrestrial field fluctuated rapidly. He described these periods as "magnetic storms." They subsequently have been related to solar activity, principally solar flares, and to the solar activity cycle as measured by a wide class of solar and terrestrial phenomenon.

More than 25 years ago, Chapman and Bartels (1) published a monumental discourse on geomagnetism and the magnetic storm. This summarized their own results, as well as the efforts of previous research workers in this very old field of scientific investigation. It also marked a decline in the interest of physical scientists in the geomagnetic field, for modern physics was then beginning to capture the attention of the majority and the most capable research investigators. Continued studies of the geomagnetic field and its characteristic variations have been carried on by a small number of dedicated workers. The principal results of such studies are surface maps of the geomagnetic field showing its direction, magnitude, and rates of change. Such maps are

currently maintained by the hydrographic offices of different countries for use in navigation.

The advent of the satellite and space-probe era, coupled with a renewed interest in planetary physics, has led to a revolution in the study of planetary magnetism as well as to the development of an entirely new field of endeavor, space physics. In this article I shall principally discuss results obtained from measurements of the Earth's magnetic field by satellites and space probes since 1958. As will become evident from these results, a totally new view of the terrestrial field emerges: one which permits the further development and investigation of many classical problems in geophysics, including magnetic storms, aurora, and the newly discovered radiation belts. In addition, it appears that a unique natural laboratory is now available in which to study various phenomenon in the broad field of plasma physics, particularly "collisionless" plasmas.

Satellites have provided direct measurements of magnetic fields in space, principally the distant terrestrial field. These data have been obtained both from satellites orbiting only a few hundred kilometers above the Earth's surface and from satellites with highly eccentric orbits penetrating more than 2.5×10^6 kilometers into interplanetary space. The interpretation of such data depends critically on the accuracy of the measurements. These data provide a relatively straightforward general description of the magnetic field. However, to understand the physics associated with the current state of the geomagnetic field it is necessary either directly or indirectly to incorporate the effects of the motion of charged particles. Indeed, the importance of the geomagnetic field today can be compared to the original motivation for its study more than 300 years ago. At that time navigation of commercial shipping was of great significance. Today the motion of charged particles as "guided" by the magnetic field in space is the "navigation" property of interest.

The Solar Wind

A discussion of the external geomagnetic field must begin not with the Earth but rather with the Sun and the phenomenon of the "solar wind." The configuration of the outermost field lines of the distant geomagnetic field, as well as the interplanetary magnetic field, is dominated by this solar plasma flux.

The concept of a solar plasma flux was introduced by Chapman and Ferraro in the early 1930's in their studies of magnetic storms [reviewed by Chapman (2)]. They postulated that after a solar flare the Sun emitted an electrically neutral but ionized "gas" which interacted with the geomagnetic field. The solar plasma compressed and temporarily confined the field to a region of space referred to as the Chapman-Ferraro geomagnetic cavity. This plasma flow was considered to be a transient phenomenon, and it was not until early in the 1950's that continual emission of substantial solar plasma was seriously considered. Biermann (3), in studying the characteristics of type I comet tails, which contain ionized constituents such as CO^+ , postulated a continuous and substantial solar corpuscular flux. This was necessary to explain the observations that comet tails are directed away from the Sun and ionized. In the late 1950's, in studies of the expansion of the solar corona, Parker (4) and Chamberlain (5) proposed different theoretical models ac-

ording to which the flux was best described as either the solar wind or the solar breeze, depending upon the predicted velocity of the radial plasma flow. Direct measurements in space have confirmed the solar-wind theory as proposed by Parker [summarized by Parker (6)]. Figure 1 shows the velocity results for isothermal coronal expansion as dependent on coronal temperature and radial distance from the Sun. It is seen that beyond a few solar radii the solar-wind velocity is approximately constant. Direct measurements in space yield velocities in the range 3 to 7×10^7 centimeters per second [Bridge *et al.* (7); Snyder and Neugebauer (8)] and densities in the range 3 to 70 protons per cubic centimeter. The concept of the solar wind as a continuous solar plasma flux is important in a study of the present state of the geomagnetic field because of the far reaching-effects of the interaction of the solar wind with the geomagnetic field.

The Magnetosphere and Its Boundary

The continual flux of solar plasma confines the geomagnetic field to a region of space which is now referred to as the magnetosphere. Less than 3 years ago, Hines (9) presented an article on the boundary of the magnetosphere entitled "The magnetopause: a new frontier in space." Rapid advances in experimental results, coupled with theoretical studies, have shown that the

confined and highly distorted geomagnetic field offers a number of new problems as well as possible solutions to many familiar ones in terrestrial and extraterrestrial physics. Figure 2 is a simplified illustration of the interaction of the solar wind with the geomagnetic field, as suggested prior to 1962. The rarefied solar plasma, consisting principally of protons of approximately 1000 electron volts energy with approximately 5 percent helium ions, is shown to interact with the geomagnetic field as a collection of separate particles. The magnetic field turns the particles around, reflecting the plasma flow, and an effective electrical current is developed on the boundary.

Since 1958, satellites have measured the distorted geomagnetic field within the magnetosphere, as well as its boundary characteristics. The measurements show that because of the flux of the low-energy plasma from the Sun and its interaction with the geomagnetic field, extraterrestrial space can be divided into three regions: (i) The interplanetary region where the properties of the interplanetary medium are undisturbed by the presence of the Earth and its magnetic field; (ii) the magnetosheath or interaction region associated with the impact of the solar wind on the geomagnetic field; and (iii) the magnetosphere, that region containing the geomagnetic field and encompassing the Earth (the geomagnetic cavity, according to the concept of Chapman and Ferraro).

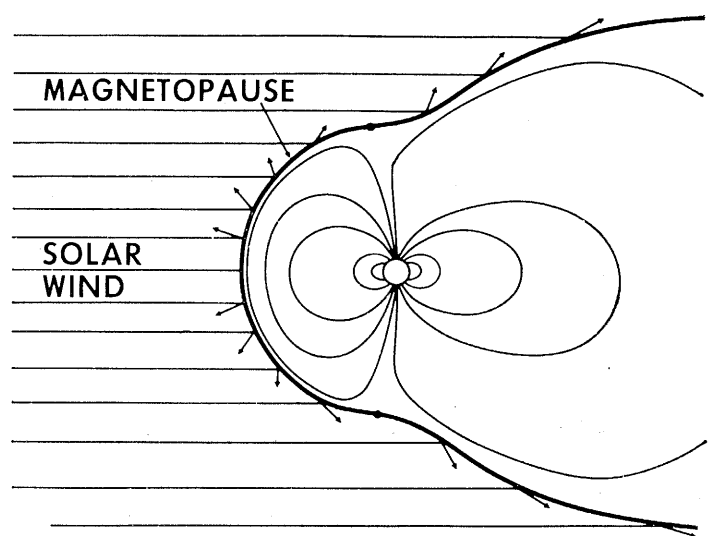
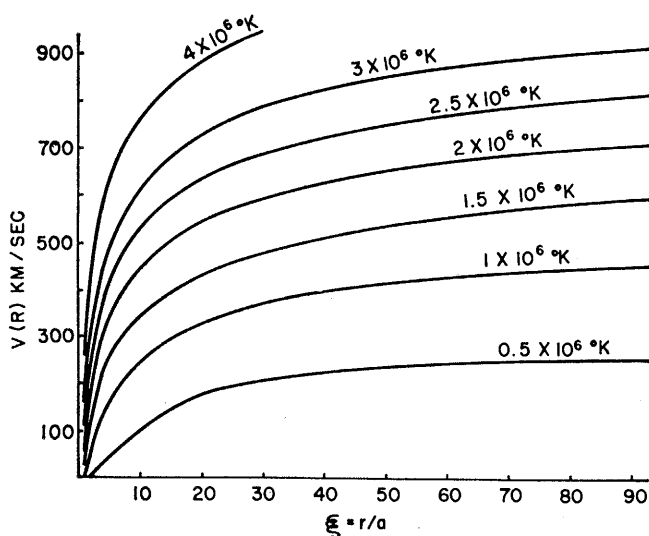


Fig. 1 (left). Theoretical results of the magnetohydrodynamic expansion of the solar corona into interplanetary space, the "solar wind" (Parker, 6). The radial velocity [$v(R)$] of the expansion as a function of radial distance (r) from the Sun in units of solar radii (a) is shown for various temperatures of the corona. Fig. 2 (right). Simplified representation of the interaction of the rarefied solar-wind plasma with the geomagnetic field. Direct impact of the plasma, as represented by individual particles, with the magnetic field is shown specularly reflected from the boundary of the geomagnetic field, which is distorted by this plasma flow.

Table 1. Summary of U.S. and U.S.S.R. satellites and space probes that have provided data on the geomagnetic field.

Satellite	Launch date	Inclination*	Lifetime (days)	Range (γ)†	Sensitivity‡	Distance§ (R_e)
Sputnik III	5-15-58	65°	30	$<6 \times 10^1$	5%	<1.3
Pioneer I	10-11-58	Earth impact	1	$<10^2$	1%	3.7-7.0
Lunik I	1-2-59	Solar orbit	1	<6000	200 γ	3-6
Explorer VI	8-7-59	47°	61	$<2 \times 10^1$	3%	2-7.5
Lunik II	9-12-59	Lunar impact	33.5 hr	<1500	50 γ	3-6
Vanguard III	9-18-59	33°	85	$10^4-6 \times 10^1$	4 γ	<1.8
Pioneer V	3-11-60	Solar orbit	50	$<10^2$	0.05-5 γ	5-9
Explorer X	3-25-61	33°	2.2	$30-5 \times 10^2$	3 γ	1.8-7
				± 50	0.3 γ	6-42.6
Explorer XII	8-16-61	33°	112	± 500	10 γ	4-13.5
Explorer XIV	10-3-62	33°	300	± 250	5 γ	5-16.5
Alouette	9-29-62	80°	Still transmitting	$<6 \times 10^1$	0.3%	1.17
Explorer XV	10-27-62	18°	90	± 4000	40 γ	1.7-4.0
Explorer XVIII (IMP I)	11-27-63	33°	181	<300	± 0.25	<32
				<40		
Electron 2	1-30-64	61°	90	<120	2 γ	3-11.6
				<1200	20 γ	
Cosmos 26	3-18-64	49°	194	$<7 \times 10^1$	$\pm 4 \gamma$	~ 1.05
Electron 4	7-11-64	61°	?	<240	?	3-11.4
				<1200		
OGO-A	9-5-64	31°	Still operating	<500	$\pm 3 \gamma$	3.8-24.3
Explorer XXI (IMP II)	10-4-64	34°	150	<300	$\pm 0.25 \gamma$	6-15.9
				<40		
Cosmos 49	10-24-64	49°	?	$<7 \times 10^1$	$\pm 4 \gamma$	~ 1.05
Mariner IV	11-28-64	Solar orbit	270	<370	$\pm 0.7 \gamma$	>10
Explorer XXVI	12-21-64	20°	Still operating	$<2 \times 10^2$	$\pm 2 \gamma$	2.5-5.1
Explorer XXVIII (IMP III)	5-29-65	33°	Still operating	<300	$\pm 0.25 \gamma$	<42
				<40		

* Inclination of orbital plane to equator. † Dynamic range of instrumentation ($1 \gamma = 10^{-2}$ oersted). ‡ Not accuracy. § Geocentric radial distance at which data was obtained.

Separating these regions are two surfaces whose physical characteristics have only recently begun to be investigated: These are the collisionless magnetohydrodynamic shock wave surface, which separates the undisturbed interplanetary medium from the magnetosheath, and the magnetopause, which separates the interaction region from the magnetosphere.

Here I shall discuss only the magnetosphere and its boundary layer, the magnetosheath. A summary of all satellites and space probes that have carried magnetometers for the explicit purpose of measuring fields in space is given in Table 1. Those experiments which have yielded data mainly on the geomagnetic field are included, along with the pertinent parameters of the experiment and characteristics of the spacecraft's orbit. Projected on the plane of the ecliptic in Fig. 3 are the relative positions of these satellite orbits with respect to the Earth-Sun line. The positions of the magnetosphere boundary and the shock-wave surface are also shown.

Distortion of the Field

Although early measurements on the Pioneer I and V satellites (10) in 1959 suggested that the regular geomagnetic field ends at approximately 14 earth

radii (R_e), no continuous traversal of the boundary was observed, because the satellite transmitted data only intermittently. Less than 5 years ago the first experimental evidence on the confinement of the geomagnetic field and observations of its boundary were ob-

tained in the experiments of Heppner *et al.* (11) and Bonetti *et al.* (12) carried out by Explorer X. This satellite, launched in March 1961, transmitted useful information only to the apogee of its first orbit. However, these data revealed a large-scale distortion of the

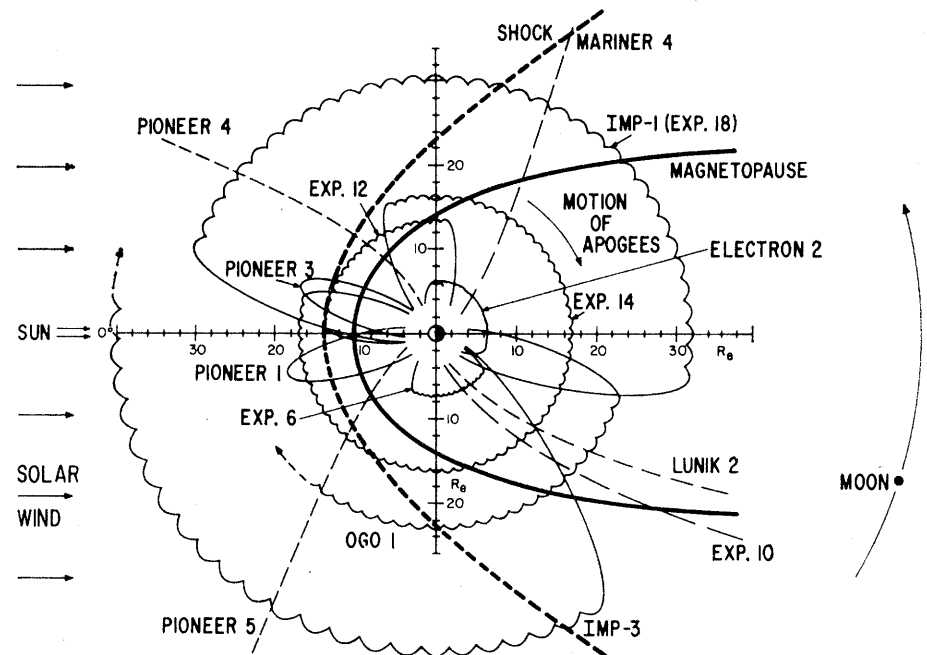


Fig. 3. Presentation of the trajectories of satellites and space probes, projected on the ecliptic plane, which have sampled the distant terrestrial magnetic field and that between Earth and the orbit of the Moon. Included also are the relative positions of the boundary of the regular geomagnetic field and the detached collisionless bow shock wave. The position of the Moon is shown in proper scale in earth radii (R_e).

geomagnetic field on the antisolar side of the Earth.

Earlier detailed mapping of the geomagnetic field close to the earth by Explorer VI (13) in 1959 had yielded data initially interpreted as indicating the existence of a permanent "ring current," due to charged particles in regular axially symmetric motion around the Earth at distances of 8 to 10 R_e . (The magnetic field of such a current system is directed opposite to the Earth's field at distances $< 8 R_e$ and parallel with the geomagnetic field at distances $> 10 R_e$.) However these measurements yielded only a component of the field and not the complete vector, so a unique interpretation was impossible. Subsequently the Explorer VI data were reexamined and shown to be consistent with the general distortion of the geomagnetic field indi-

cated by Explorer X and later satellite measurements (14). Measurements of the distant terrestrial magnetic field made by the Russian Moon probes Luniks I and II detected large depressions of the main field at 2.8 to 4.0 R_e (15). Recently the Russian Electron II earth satellite (16) has also confirmed, in approximately the same region, smaller depressions of the field than those observed on previous Soviet launches. Direct particle measurements in the radiation belt (17) do not reveal particle fluxes great enough to explain the magnetic-field data in terms of a ring current. The magnetic-field data must be interpreted in terms of a permanent, non-axially symmetric distortion of the magnetosphere so that the local time of data observations must be considered.

Shortly after Explorer X, in August 1961, the United States launched Ex-

plorer XII, the first in a series of increasingly sophisticated satellites to investigate various particle, field, and plasma phenomena in the geomagnetic field and interplanetary space. These measurements (18, 19) showed a termination of the compressed geomagnetic field at a distance between 8 and 10 R_e on the sunlit side of the Earth and simultaneous termination of the Van Allen trapping region for energetic particles. In addition, an increased plasma flux, inferred to be thermalized solar plasma, was observed beyond the magnetosphere. These particle and field measurements, combined with the data from Explorer X, established the permanent existence of a confined and compressed geomagnetic field.

The relative positions of the magnetosphere and its boundary layer as measured by Explorer XII are shown in

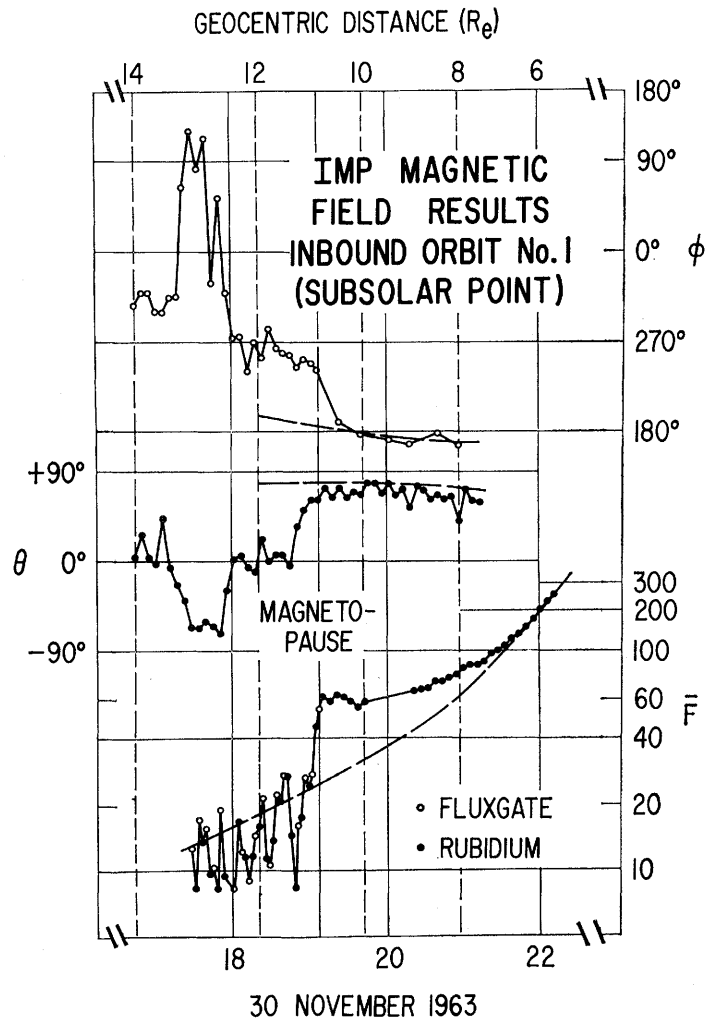
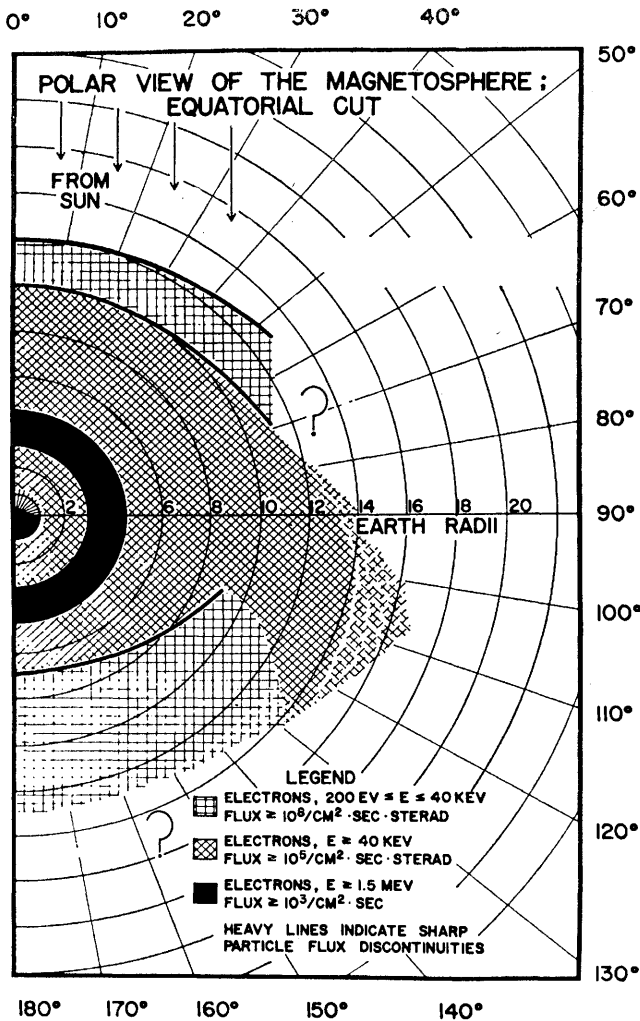


Fig. 4 (left). Energetic-particle measurements obtained from Explorer XII in 1961 by Freeman (19). The relative positions of the various regions surrounding the Earth, as defined by the energetic-particle detectors, are projected on the Earth's equatorial plane. Among these regions are the Van Allen radiation belts.

Fig. 5 (right). Magnetic field measurements of the distant geomagnetic field from IMP-I inbound on orbit No. 1, 30 November 1963. The abrupt discontinuity in magnitude and direction of field at 10.8 R_e is identified as the magnetosphere boundary. Theoretical values for the magnitude of the field (F), ϕ , and θ are shown as dashed curves.

Fig. 4. These data are projected on the equatorial plane of the Earth and show the roughly spherical shape of the magnetosphere boundary near the subsolar point, and also the limited extent of the thermalized plasma. It was also possible with these direct measurements of the boundary position to place in a proper perspective the earlier measurements by the Pioneer and Explorer satellites (20).

A comprehensive survey of the confined geomagnetic field and its boundary and, significantly, magnetic measurements at the collisionless shock wave have been made by Explorer XVIII (IMP-I) (21, 22). The magnetic-field measurements, as presented in Fig. 5 on the orbit that passed nearest the subsolar point on the magnetosphere boundary (23).

The Boundary

It is seen that the observed magnetic field within the magnetosphere is directed parallel to that theoretically predicted. The magnitude of the field increases abruptly within the magnetosphere boundary and gradually approaches the theoretical value near the Earth. The disturbances and rapid fluctuations of the magnetic field observed beyond the magnetosphere boundary are typical of what has been observed in that region. Plasma measurements obtained by the same IMP-I satellite (7) have shown a remarkable correlation with the position of the magnetosphere boundary. An approximately isotropically directed flow of plasma immediately beyond the boundary is generally observed.

The magnitude of the field at the magnetosphere boundary is approximately twice that which would be due to the Earth alone. This is understood by considering the diamagnetic effects of the plasma, which must compress and thereby exclude the terrestrial magnetic field so that the normal component at the boundary is zero. An image dipole on the solar side of the magnetopause with the same value as the Earth's dipole will yield a zero normal component at a plane boundary approximating the magnetopause. At the boundary it will lead to a doubling of the field magnitude. More detailed computations of the shape of the magnetosphere boundary have been conducted by a number of investigators,

and are summarized by Beard (24). In general they employ the simplified model shown in Fig. 2. There has been some discussion about the physical character of the reflection of plasma at the boundary, but the results are mutually in good agreement. The mathematical problem solved is one in which the boundary conditions are known but the position of the boundary is to be deduced. This represents a variation to the classical boundary-value problems which are familiar in mathematical physics.

It is possible to estimate the distance at which the geomagnetic field will terminate by consideration of the balance of magnetic pressure, P , and plasma momentum flux at the subsolar point. If B_0 is the equatorial field strength of the Earth, n is the density of the plasma, V_s is the velocity of the solar wind, B_{11} is the total field at the magnetosphere boundary, and R_b is the geocentric radial distance to the magnetosphere boundary, then

$$P = 2mnV_s^2 = B_{11}^2/8\pi$$

but

$$B_{11} = 2B_0 (R_e/R_b)^3$$

thus

$$R_b = R_e [B_0^2/4\pi mnV_s^2]^{1/2}$$

Substituting $B_0 = 0.312$ gauss, $n = 2$ to 10 protons per cubic centimeter, and $V_s = 4 \times 10^7$ cm/sec yields $R_b = 8$ to $11 R_e$, which is in reasonably good agreement with observations.

The magnetic field measurements obtained when IMP-I was outbound on orbit No. 1 at an angle of 45° to the Sun-Earth line are shown in Fig. 6. As before, the magnitude of the field is above that theoretically predicted within the magnetosphere, and at $11.3 R_e$ the magnitude decreases abruptly as the directional character of the field changes to rapidly fluctuating. Higher-frequency fluctuations are inferred from the separate presentation of the root-mean-square deviations of the X_{se} , Y_{se} , and Z_{se} components of the field. At a distance of $16.8 R_e$, the average magnitude of the field approaches 5 gammas (5×10^{-5} oersted), and the direction of the field stabilizes. At the same time, the high-frequency fluctuations disappear. This change in character of the field is identified as representing the detached bow shock wave which develops in the supersonic flow of the solar wind as it interacts with the geomagnetic field (25).

The Interplanetary Medium

The interplanetary medium contains an average magnetic field of approximately 5 gammas (22), and its density is only a few protons per cubic centimeter, so that the phase velocities in the plasma, that is, the Alfvén ve-

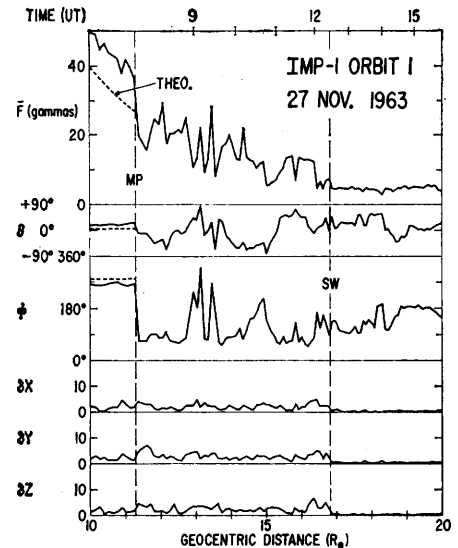


Fig. 6. Magnetic field results on the outbound portion of orbit No. 1 from IMP-I, 27 November 1963. Clearly evident are the magnetosphere boundary at $11.3 R_e$ and a termination of the rapid fluctuations of the magnetic field at $16.8 R_e$ identified as the collisionless shock wave.

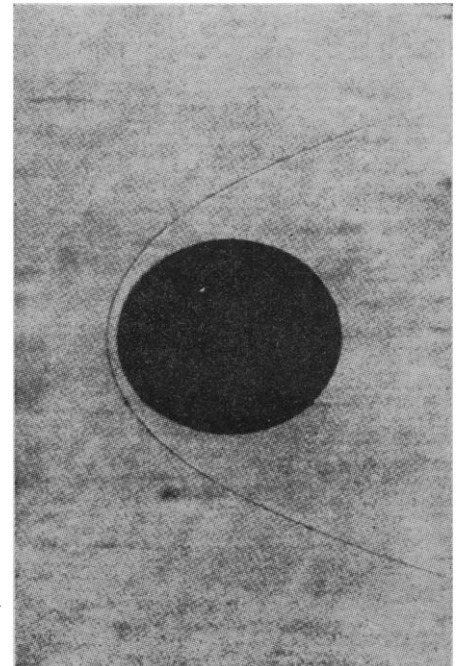


Fig. 7. Rotating mirror shadowgraph of high-speed aerodynamic flow (from left) and the detached bow shock wave surrounding a sphere at Mach number 14.

locities, are approximately 5×10^6 centimeters per second. Since the solar wind flow is both deduced (26) and measured (7, 8) to be at least 3×10^7 centimeters per second, the corresponding Alfvén Mach number of the flow

is at least 6. The characteristic feature of the magnetic field as illustrated in Fig. 6, in which the three regions of space defined at the beginning of this article are so clearly identified, is in general observed clearly in each radial

traversal of the geomagnetic field while the satellite is passing on the sunlight side of the earth.

Present interpretations of the interaction of the solar wind with the geomagnetic field are based on an analogy with hypersonic gas dynamics. An excellent review of the arguments for this analogy has been presented by Levy, Petschek, and Siscoe (27). For reference, Fig. 7 shows a sphere interacting in a hypersonic gas flow at Mach number 14. This shadowgraph shows the development of a discontinuous change in physical properties along the roughly parabolic surface, indicated by the heavy line enclosing the sphere. It is important to recognize that it is not the Earth but rather its magnetosphere which represents a blunt object (approximately spherical on the portion around the sunlit hemisphere) and which interacts with the solar wind flow to develop the detached bow shock wave.

A direct comparison of the theoretical shape and position of the shock with observations is shown in Fig. 8. The positions of the shock and magnetosphere boundary are represented by dots and crosses, respectively. The solid lines which pass through the dots and crosses represent the theoretical prediction (28) for both the magnetosphere boundary and the detached bow shock wave. The theoretical standoff ratio (a measure of the thickness of

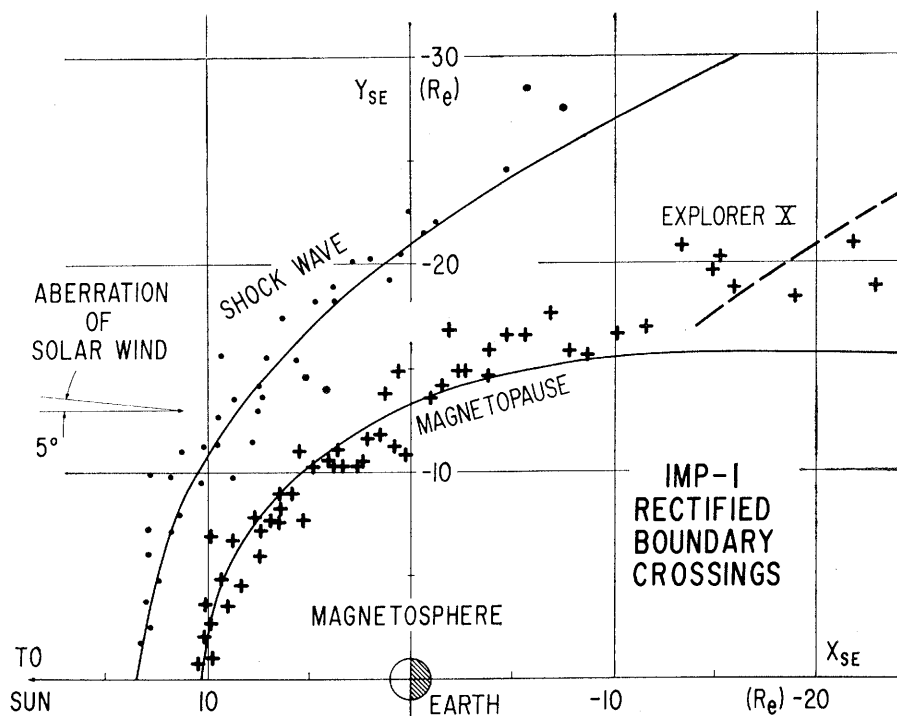


Fig. 8. Comparison of the IMP-I shock wave and magnetosphere-boundary crossings with the gas-dynamic shock model of Spreiter and Jones (28). Spreiter and Jones's results, shown as solid lines projected on the ecliptic plane, have been adjusted to match the observed standoff ratio. The observed shape of the shock wave closely matches the predicted shape.

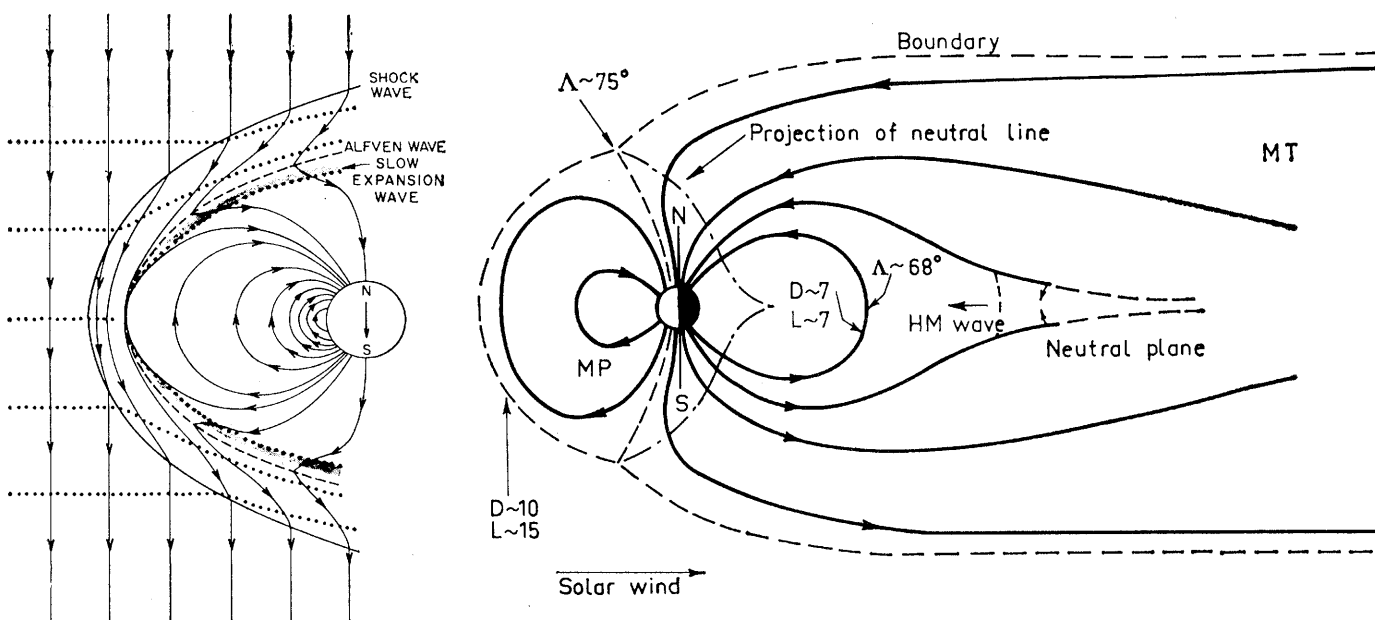
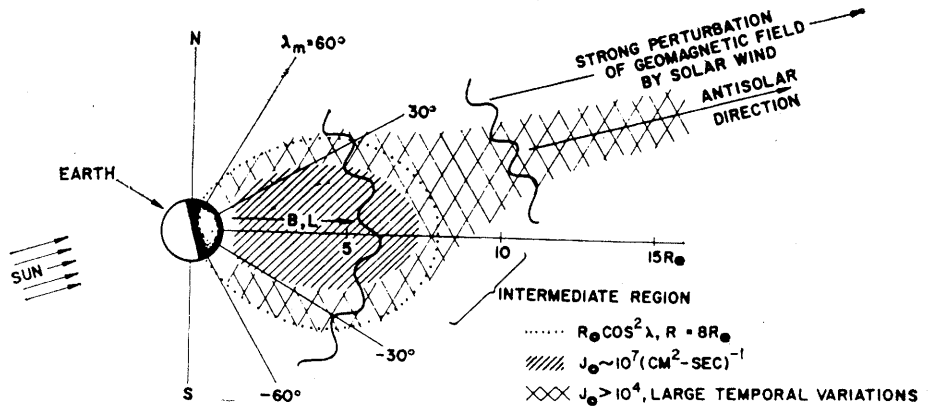


Fig. 9 (left). Schematic drawing of magnetic field (solid lines) and plasma flow (dots) in the subsolar region. The flow is decelerated by the bow shock. The magnetosphere boundary is resolved into an Alfvén wave and a slow expansion fan (after Levy *et al.*, 27). Fig. 10 (right). Schematic diagram of the geomagnetic field as distorted by the solar wind, showing lines of force in the noon-midnight meridian plane. The "open" tail comprises two bundles of field lines emerging from the polar caps centered at geomagnetic latitudes of about 87° on the midnight meridian (after Piddington, 35).

Fig. 11 (right). Schematic diagram of the spatial distribution of electrons (energy > 40 kev) as obtained from Explorer XIV measurements near the midnight meridian plane in 1963. J , directional flux of electrons (Frank, 32).



the magnetosheath) has been slightly adjusted to provide a better agreement between observations and theory. In the gas-dynamic analogy this means increasing the equivalent specific-heat ratio above the assumed value of 5/3.

Several studies of the precise mechanism leading to the development of a collisionless shock wave, with specific application to the case of the interaction of the solar wind with the geomagnetic field, have been conducted (29). Although the details are not well understood, the observations strongly suggest the existence of a shock wave or at least a shock-like phenomenon in which the characteristics of the solar wind and the interplanetary magnetic field abruptly change upon penetrating the magnetosheath. The strength of the magnetic field is increased, the field becomes turbulent, the directed solar-plasma flow is randomized, and the spectrum is broadened.

The gross physical characteristics at the boundary of the magnetosphere have been measured by a number of satellite experiments. An important finding has been that the magnetosphere boundary is extremely narrow. With the assumption that the position of the boundary while it is traversed by the satellite, is fixed, the thickness of the magnetopause is found to be $\approx 2 \times 10^7$ centimeters, a very small fraction of an earth radius. Levy *et al.* (27) have analyzed the problem of the detailed characteristics of the magnetopause boundary layer surrounding the magnetosphere, as shown in Fig. 9. They consider the magnetopause as an Alfvén wave and a slow expansion wave which are coincident near the subsolar point but which separate near

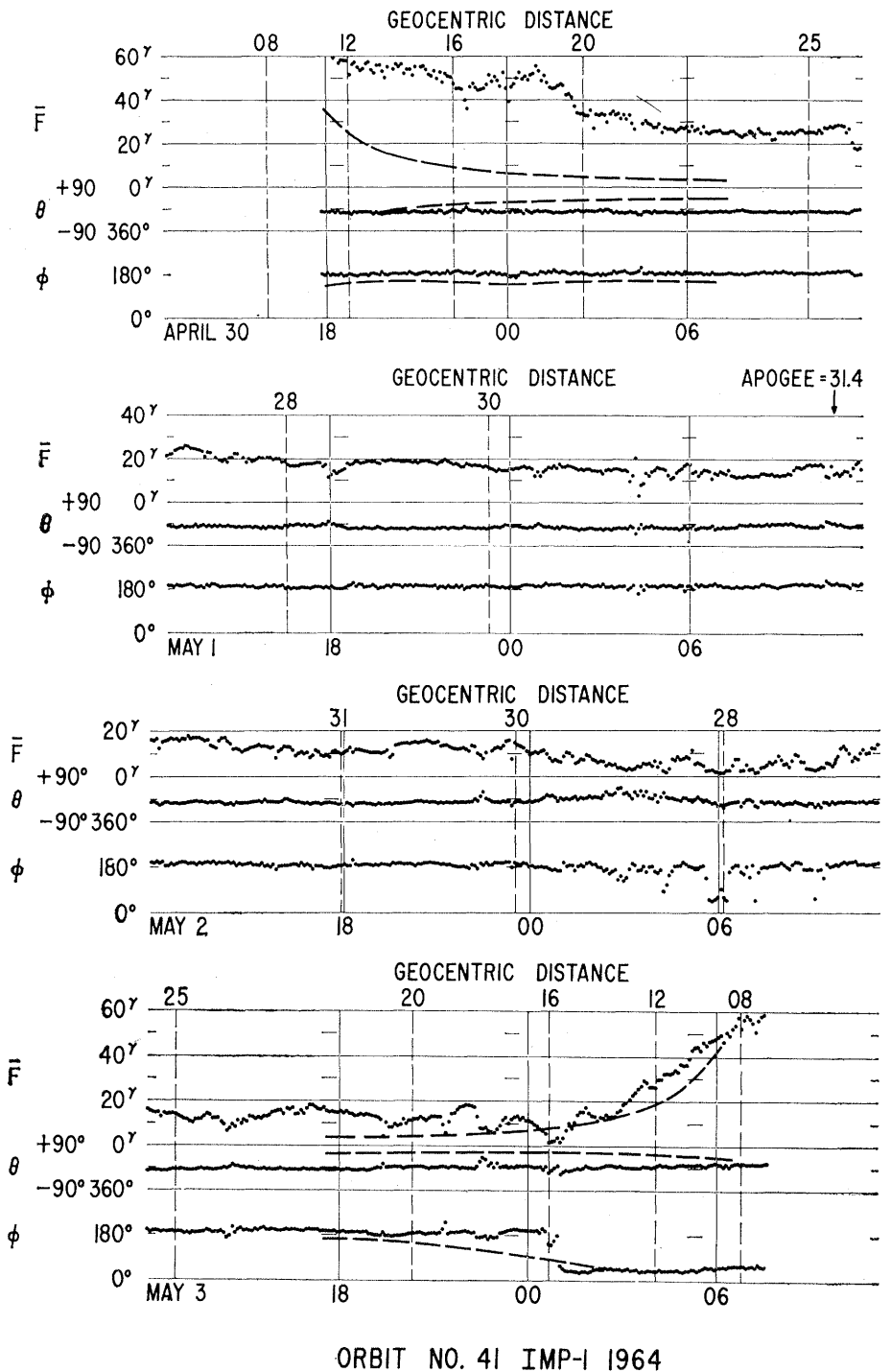


Fig. 12 (right). Measurements of the Earth's magnetic tail field near the midnight meridian plane by IMP-I on orbit No. 41, 30 April to 4 May 1964. The direction of the field is observed to closely parallel the Earth-Sun line with a rapid change from antisolar to solar direction on the inbound pass at a radial distance of $16 R_E$. This is interpreted to represent traversal of the magnetic neutral sheet in the Earth's magnetic tail and is characteristic of observations of this phenomenon by IMP-I (Ness, 34).

the polar regions. In addition, as originally noted by Dungey (30), there is every reason to anticipate that high-latitude geomagnetic field lines will be connected with the interplanetary magnetic field as shown in Fig. 9. This connection has further implications for the configuration of the field on the night side of the Earth. Satellite measurements at present are not sufficiently definitive to ascertain whether the model as proposed is valid or indeed to

what extent connection exists on the sunlit hemisphere of the magnetosphere.

The Earth's Magnetic Tail

In a 1960 study of the phenomenon of the geomagnetic storm, Piddington (31) suggested that magnetic field lines would temporarily be extended on the night side of the Earth somewhat as

shown in Fig. 10 and would be distorted by an effective viscous stress of the solar wind on the outermost lines of force. The first measurements of the magnetic field on the night side of the Earth at great distance by Explorer X in 1961 indicated that such a distortion existed even in the absence of a geomagnetic storm. Subsequently Explorer XIV (32) revealed, near local midnight, an apparent electron "tail," as shown in Fig. 11, in the distribution of energetic particles. Using data from the same satellite, Cahill (33) measured the terrestrial field approaching an approximately antisolar direction at a distance of $16 R_e$. Recent detailed measurements of the Earth's magnetic field on the night side, made by IMP-I (34), have shown that the geomagnetic field trails out far behind the Earth at least halfway to the Moon and forms a substantial and permanent magnetic tail.

That such an appendage to the geomagnetic field would exist permanently has recently been predicted (35-37). A magnetically neutral region separating oppositely directed fields has been detected (34) and is illustrated as the neutral plane in Fig. 10. In the model of Dessler (36), the Earth's magnetic field trails out to 20 to 50 astronomical units behind the Earth, following the direction of the flow of plasma. Dessler also proposes negligible merging of field lines across the neutral plane from the upper and lower regions of the tail. An alternative view has been taken by Axford *et al.* (37) on the basis of initial suggestions by Dungey (30) in which an appreciable merging of field lines on the night side of the earth would lead to the development of a neutral line and sheet region which would contain enhanced particle fluxes, such as those observed by Explorer XIV.

Detailed measurements from IMP-I on orbit No. 41 in May 1964 yielded data obtained when the satellite was closest to the midnight meridian plane (Fig. 12). These data demonstrate that the direction of the field is closely parallel to the Earth-Sun line ($\theta = 0^\circ$ and $\Phi = 0^\circ$ or 180°) and that the field is directed either toward ($\Phi = 0^\circ$) or away ($\Phi = 180^\circ$) from the Sun, depending upon whether the satellite is above or below the magnetically neutral region identified as the neutral sheet. Shown in Fig. 12 on the inbound portion of the orbit is the abrupt change in the direction of the magnetic field at $16 R_e$. Although the satellite motion is predominantly radial there is also a slight transverse motion, so that

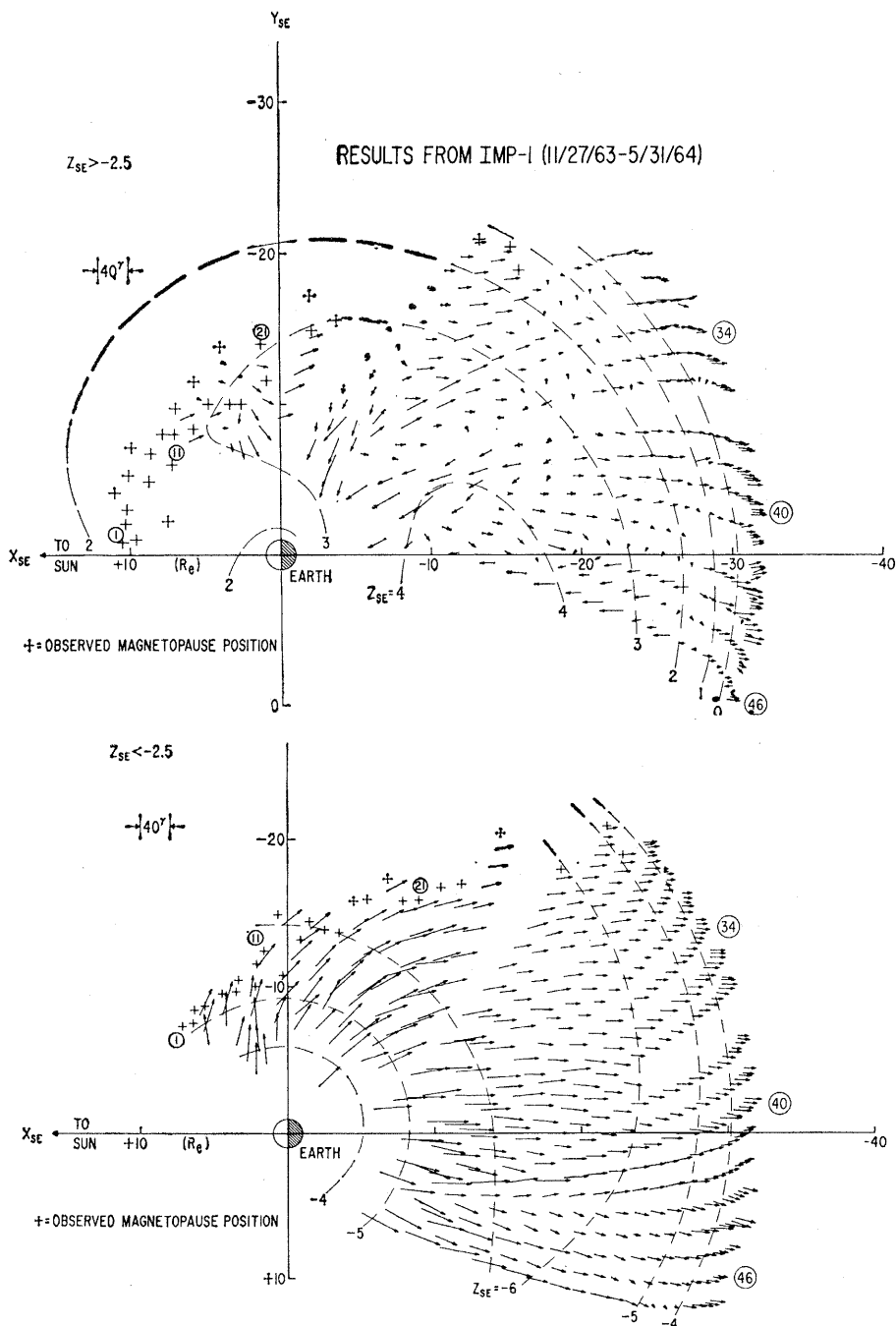


Fig. 13. Summary of the averaged hourly measurements of the XY component made in 1964 by IMP-I while in the Earth's magnetic tail. The lower portion of the figure corresponds to measurements performed while the satellite was more than $2.5 R_e$ below the ecliptic plane; the upper portion corresponds to positions of the satellite above this. Clearly evident is the distortion of the geomagnetic field forming the extended geomagnetic tail (Ness, 34).

the apparent thickness of the transition across the neutral sheet implies an extremely thin feature in the Earth's magnetic tail.

A summary of the IMP-I observation of the magnetic tail is presented in Fig. 13, in which the XY components of the magnetic field are projected on the ecliptic plane. This presentation, with little distortion, presents a correct view of the geomagnetic tail field. The data are separated to show the results obtained when the satellite is above or below an imaginary plane at $2.5 R_e$ below the ecliptic (chosen for clarity of presentation). In this figure it is possible to follow the individual orbits of the satellite and to identify a single or indeed multiple traversal of the neutral sheet on each orbit. Multiple traversals of the neutral sheet are interpretable in view of the "wobble" of the Earth's magnetic dipole axis once every 24 hours and the associated orientation of the magnetic neutral sheet (34).

The general interpretation of the observations is that lines of force originating in the polar cap regions of the Earth are distorted by the solar wind to trail out far behind the earth and form the magnetic tail (see Fig. 14). On this basis it is possible to predict the colatitude of the polar cap region which will correspond to the observed characteristics of the magnetic tail field. Let R_t be the radius of the tail, B_t the magnitude of the tail field, and θ_{pc} the colatitude of the polar cap region. Then conservation of flux or connection of field lines between the polar cap and the tail requires that

$$B_t = 4B_0 (R_e/R_t)^2 \sin^2 \theta_{pc}$$

Substituting a value of 16 gammas, obtained from the IMP-I measurement, for the median magnitude of the field in the tail (38) and a value of $22 R_e$ for the approximate radius of the tail (34) yields a predicted polar cap region of approximately 14° colatitude. This corresponds well with the polar cap region defined by the auroral zone and

Fig. 15 (right). Comparison of worldwide magnetograms during the sudden commencement of geomagnetic storm, which began 10 May 1964 at 0035 UT, with magnetic-field measurements by IMP-I in the Earth's magnetic tail. The simultaneous worldwide increase at the onset of the storm is correlated positively with an increase in field strength at a distance half-way to the Moon. The subsequent main-phase decrease is accompanied by an additional increase in tail field magnitude (Behannon and Ness, 38).

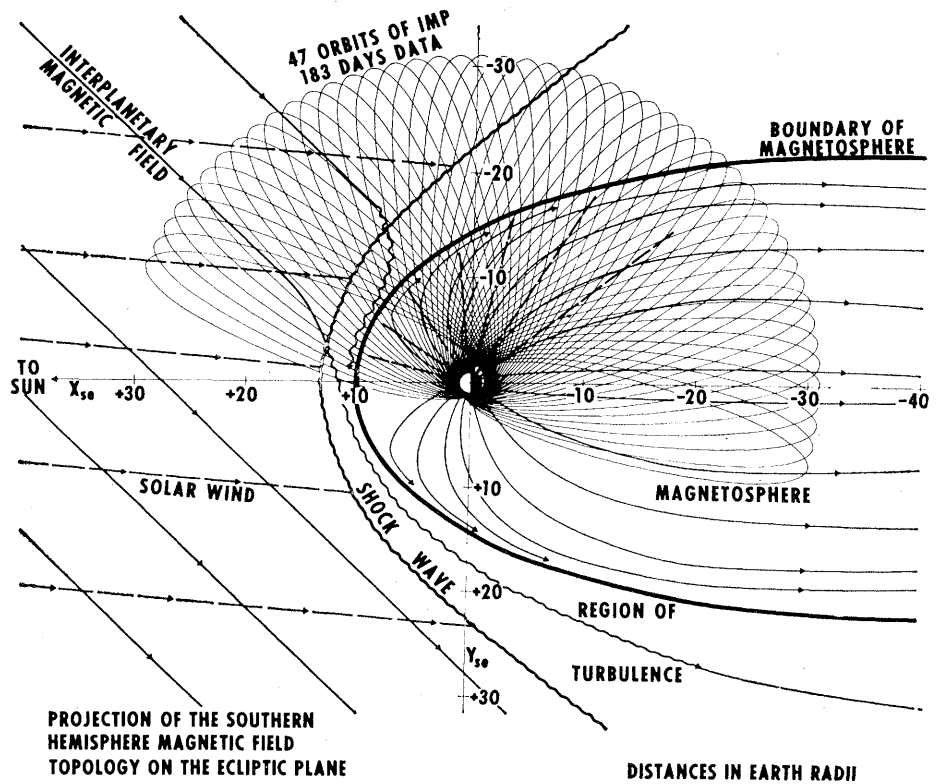
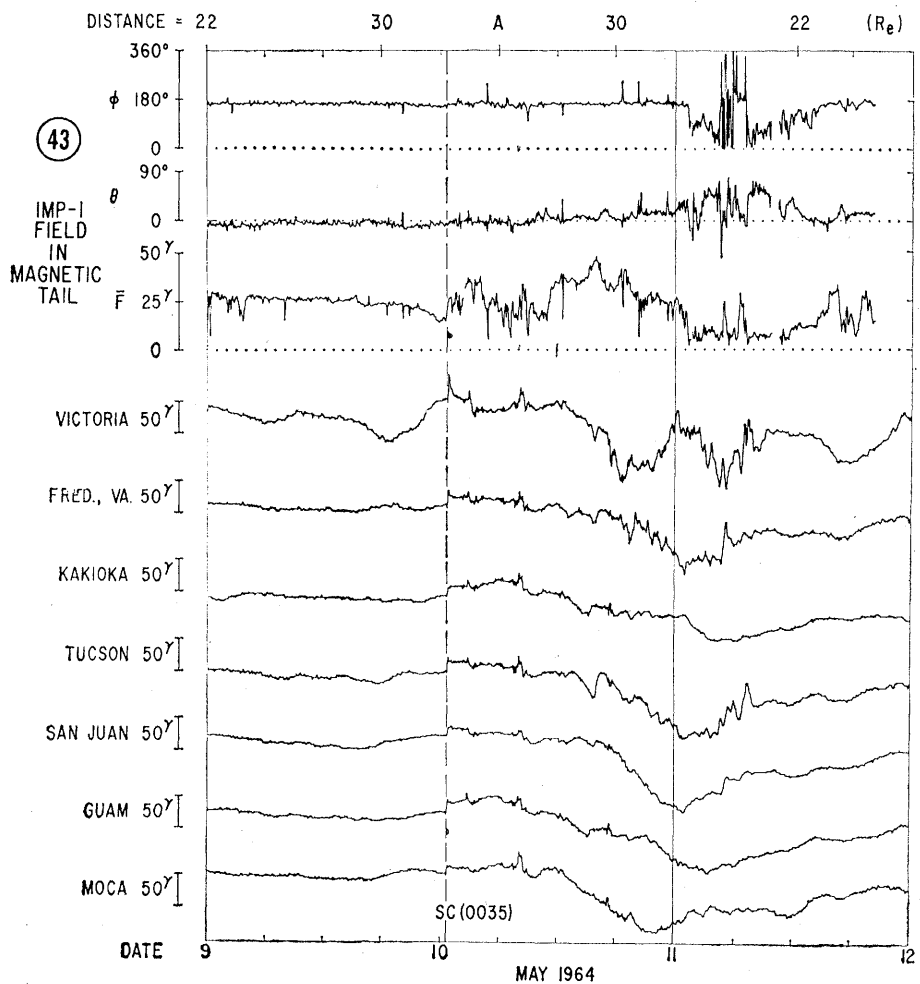


Fig. 14. Schematic illustration summarizing the results projected on the ecliptic plane, of the IMP-I magnetic-field experiment, 27 November 1963 to 31 May 1964. The direction of the interplanetary magnetic field is observed to be approximately 45° to the direction of flow of the solar wind. Indicated are the relative positions of the satellite during the 6-month period during which the measurements were performed (Ness, 34).



also with the boundaries of the trapped-radiation belts. The observations of the radiation belt have shown that there is a strong day-night asymmetry in the invariant latitude at which the trapped particles terminate; thus the distortion suggested in Fig. 10 is substantiated. Measurements of intense particle fluxes at latitudes higher than the radiation belts (39) suggest that their origin is within the geomagnetic tail. It appears plausible that the tail is the source of the energetic particles that form the aurora (40). However, the exact mechanisms for acceleration of solar plasma particles to auroral energies are not clear.

Magnetic Storms

The theoretical study of magnetic storms originally led to the suggestion that the transient flux of plasma from the sun compresses the geomagnetic field and leads to the initial increase in the horizontal component of the geomagnetic field (*I*). Subsequently the solar particles were trapped in the geomagnetic field in a "ring current" which then led to the main phase decrease of the terrestrial field for a day or so afterwards. This ring current then decayed, and the geomagnetic field resumed its normal configuration. With the recent measurements of a continual

plasma confinement of the geomagnetic field and the permanent existence of the Earth's magnetic tail, revisions of these concepts are necessary.

Several magnetic storms occurred while measurements were being made in the magnetic tail by IMP-I. One on 10 May 1964 has the characteristic initial sudden increase in the horizontal component followed by a decrease and recovery over several days (see Fig. 15). Correlated with the data in Fig. 15 are the magnetic-field measurements obtained in the Earth's magnetic tail. The sudden compression of the magnetosphere, possibly associated with a propagating shock wave in the interplanetary medium, was observed at 0035 U.T. on 10 May. The correlation of magnetic field variations in the tail with those on the Earth's surface corresponds to changes in pressure and tension on the distant lines of force of the magnetic field (41).

In Fig. 16 measurements of the boundary of the trapping region are compared with measurements of the Earth's magnetic tail field during a magnetic storm in April 1964 (42). The trapping boundary was measured at an elevation of 1000 kilometers by the APL satellite 1963-38C. The latitude at which the trapping boundary terminates is predicted with the use of a theoretical model of the distorted geomagnetic field which includes a tail and neutral sheet. Although there is a discrepancy between the observed and predicted positions of the trapping boundary for the particle energies observed, the changes in this boundary are coincident in time and equal in magnitude to those predicted. This lends very strong support to this tail-field topology. In addition, the planetary magnetic-activity index, *K_p* is correlated with the tail-field magnitude. Detailed studies of the tail field (38) during a 3-month period have indicated that *K_p* is generally positively correlated with tail-field magnitude and that an increase of solar-plasma flux drags additional lines of force into the Earth's magnetic tail.

Summary

The Earth's magnetic field has been mapped during the past 8 years with the most unique "laboratory benches" yet developed: satellites and space probes. They have introduced and stimulated considerable activity in the

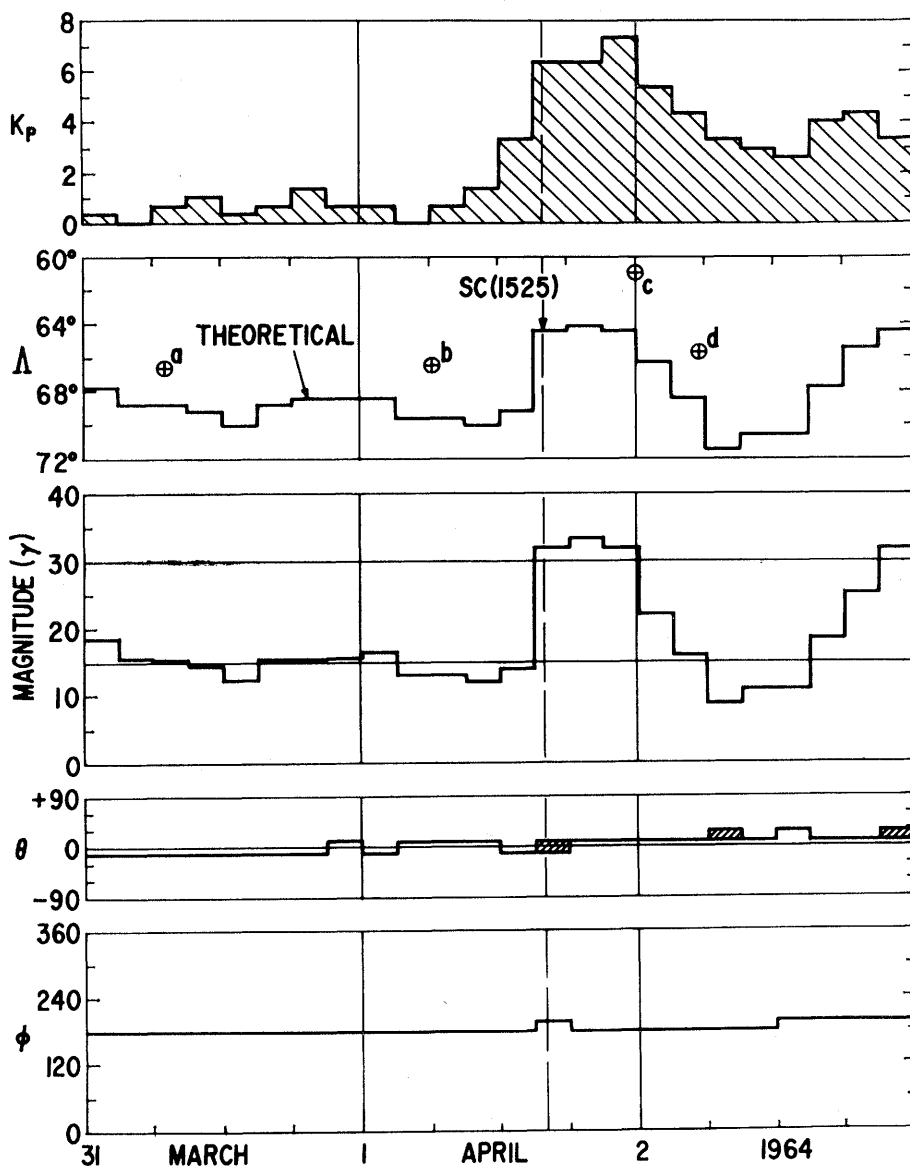


Fig. 16. Correlation of magnetic-tail measurements during the geomagnetic storm of 1 April 1964 with measurements of the trapped-radiation boundary obtained by satellite 1963-38C (Ness and Williams, 40). The invariant trapping boundary (Λ) is theoretically predicted by invoking a tail field model of the geomagnetic field and is compared directly with observations (*a* to *d*). Also included is the planetary magnetic activity index *K_p* which is positively correlated with tail field magnitude.



Fig. 17. Photograph of comet Whipple-Fedtko-Tevzadze (1943I), indicating screwlike motions in the tail. Similarity of solar wind interaction with the geomagnetic field and with the cometary coma suggests that the Earth may be compared to a "magnetic comet" with the magnetic tail and sheet corresponding to the observable ion-tail in the comet and the magnetosphere corresponding to the coma (photograph by C. Hoffmeister, Sonneberg).

new field of space physics. They have also brought to many classical geophysical problems a clear, fresh, and more accurate insight. This is particularly true in the field of geomagnetism; the Earth's magnetic field is now known to be continuously compressed by a solar corpuscular flux, the solar wind, and terminated at approximately 65,000 kilometers toward the Sun. However, the Earth's magnetic field is extended far behind the Earth in the direction away from the Sun, forming a magnetic tail. No termination of the tail at distances more than halfway to the moon is indicated. Suggested tail lengths vary from extremes of 50 astronomical units to only 1000 R_e . In a related experiment the Mariner IV space probe reports the absence of electron fluxes associated with the magnetospheric tail or wake at distances of 3000 R_e (43). At what distance the tail terminates and what is the character of the termination are problems whose answers are of great significance with respect to our study of the geomagnetic field and related terrestrial phenomenon.

Because of the similarity of the phenomenon responsible for the development of this magnetic tail feature to that responsible for the tail of a comet, the Earth may be compared to a "magnetic comet" (see Fig. 17). In this metaphor the nucleus of a comet would correspond with the Earth, the coma

with the magnetosphere, and the ionized-gas tail with the Earth's magnetic tail. Such a suggestion is admittedly rather descriptive, although future experimental and theoretical investigations may indicate a substantially more proper and complete analogy. One of the principal problems in the analogy is that there is no known mechanism for producing a large magnetic field in the comet nucleus or coma, so the mechanism of formation of the ionized gas tails is not yet clear. Capture of the interplanetary magnetic field offers the most plausible hypothesis at present.

There are two other aspects of magnetic-field studies which have not been treated here but which contribute significantly to a new view of the terrestrial field. One is the recent results obtained from Mariners II (44) and IV (45) space probes investigating the magnetic fields of Venus and Mars. Although these space probes did not make impact with the planets, they passed close enough, and contained magnetometers and energetic particle detectors sensitive enough, to estimate the strength of the planetary magnetic fields. Compared with the Earth's magnetic moment of 8×10^{25} electromagnetic units, the maximum moment of Venus is only 3.4 percent and that of Mars 0.03 percent. Thus the Earth is unique among these planets in having such a strong field.

The second group of new results pertains to the origin and history of the geomagnetic field. Any mechanism for the origin of the field must be described in relation to the present geometry and state of the Earth and its core. However, the origin of the field has eluded quantitative and explicit theories, even with modern computers capable of studying such large-scale geophysical systems. The classical theory that the field originated in a fluid core "dynamo" still has many advantages (46). The recent theory of Malkus (47), which depends on an interaction of the fluid core with the solid mantle and on the associated precessional torques, is significant in the light of recent observations in paleomagnetic research. Measurements of the remanent magnetism of rocks show that the direction of the ancient geomagnetic field has been both approximately the same as and opposite to that of the present field (48). This implies that the Earth's field has reversed itself. These reversed magnetizations are an important feature of the Earth's magnetic field in past times, and transitions from one "polarity" to the other occur over relatively short time scales.

This paleomagnetic research, coupled with satellite measurements of the present state of the Earth's magnetic field and data on the absence of magnetic fields on Venus and Mars, clearly stimulates future research on the very

unique combination of parameters which lead to the existence of the terrestrial magnetic field. The changes in polarity imply a dynamic origin, and the existence of the solar wind leads to temporal variations that depend on both the strength and direction of the field as well as on the solar wind flux. Certainly these new experimental results, when fully analyzed and incorporated into theoretical models, will make an important contribution to our concept of the origin of the solar system as it is currently observed.

References and Notes

1. S. Chapman and J. Bartels, *Geomagnetism* (Oxford Univ. Press, Oxford, 1940).
2. S. Chapman, in *Geophysics: The Earth's Environment*, C. DeWitt *et al.*, Eds. (Gordon and Breach, New York, 1963), p. 373.
3. L. Biermann, *Z. Astrophys.* **29**, 274 (1951).
4. E. N. Parker, *Astrophys. J.* **128**, 664 (1958).
5. J. W. Chamberlain, *ibid.* **131**, 47 (1960).
6. E. N. Parker, *Interplanetary Dynamical Processes* (Interscience, New York, 1963).
7. H. S. Bridge, A. Egidio, A. Lazaruns, E. Lyon, L. Jacobson, *Space Research* **5**, 969 (1965).
8. C. W. Snyder and M. Neugebauer, *ibid.* **4**, 89 (1964).
9. C. O. Hines, *Science* **141**, 130 (1963).
10. C. P. Sonett, D. L. Judge, A. R. Sims, J. M. Kelso, *J. Geophys. Res.* **65**, 55 (1960); P. J. Coleman, C. P. Sonett, D. L. Judge, E. J. Smith, *ibid.*, p. 1856.
11. J. P. Heppner, N. F. Ness, C. S. Scarce, T. L. Skillman, *ibid.* **68**, 1 (1963).
12. A. Bonetti, H. S. Bridge, A. J. Lazaruns, B. Rossi, F. Scherb, *ibid.*, p. 4017.
13. E. J. Smith, P. J. Coleman, D. L. Judge, C. P. Sonett, *ibid.* **65**, 1858 (1960); C. P. Sonett, E. J. Smith, D. L. Judge, P. J. Coleman, *Phys. Rev. Letters* **4**, 161 (1960).
14. E. J. Smith, C. P. Sonett, J. W. Dungey, *J. Geophys. Res.* **69**, 2669 (1964).
15. Sh. Sh. Dolginov, Ye. G. Yeroshenko, L. N. Zhuzgov, N. V. Pushkov, L. O. Tyurmina, *Artificial Earth Satellites* **3-5**, 490 (1960); ———, *Geomagnetism Aeronomy* **1**, 21 (1961).
16. Sh. Sh. Dolginov, Ye. G. Yeroshenko, L. N. Zhuzgov, *Space Res.*, in press.
17. R. A. Hoffman and P. A. Bracken, *J. Geophys. Res.* **70**, 3541 (1965).
18. L. J. Cahill and P. J. Amazeen, *ibid.* **68**, 1835 (1963); J. W. Freeman, J. A. Van Allen, L. J. Cahill, *ibid.* **68**, 2121 (1963).
19. J. W. Freeman, *ibid.* **69**, 1691 (1964).
20. L. J. Cahill, in *Space Physics*, D. P. LeGalley and A. Rosen, Eds. (Wiley, New York, 1964), p. 301.
21. N. F. Ness, C. S. Scarce, J. B. Seek, *J. Geophys. Res.* **69**, 3531 (1964).
22. N. F. Ness, C. S. Scarce, J. B. Seek, J. M. Wilcox, *Space Res.*, in press.
23. In a study of the interaction of the solar wind with the geomagnetic field, a coordinate system has been introduced which reflects the importance of the solar origin of the plasma. Direct measurements of the solar wind indicate velocities between 3 and 7×10^7 cm/sec. The heliocentric orbital motion of the earth through interplanetary space is only 3×10^6 cm/sec, so that the direction of the solar plasma flow shows an aberration from the Sun-Earth-line of only 3 to 6 degrees. A right-handed geocentric solar ecliptic coordinate system comprising an X_{sc} -axis directed from the Earth to the Sun and the Z_{sc} -axis normal to the ecliptic plane has been found to be a useful reference in which to study measurements of fields and plasmas. In this coordinate frame, θ is the latitude and ϕ the longitude as measured east of the Sun.
24. D. B. Beard, *Rev. Geophys.* **2**, 335 (1964).
25. W. I. Axford, *J. Geophys. Res.* **67**, 3791 (1962); P. J. Kellogg, *ibid.*, p. 3805.
26. N. F. Ness and J. M. Wilcox, *Phys. Rev. Letters* **13**, 461 (1964).
27. R. H. Levy, H. E. Petschek, G. L. Siscoe, *Am. Inst. Aeronaut. Astronaut. J.* **2**, 2065 (1964).
28. J. R. Spreiter and W. P. Jones, *J. Geophys. Res.* **68**, 3555 (1963).
29. J. G. Corday, *ibid.* **70**, 1278 (1965); P. D. Noerdlinger, *ibid.* **69**, 369 (1964); F. L. Scarf, W. Bernstein, R. W. Fredricks, *ibid.* **70**, 9 (1965).
30. J. W. Dungey, *Phys. Rev. Letters* **6**, 47 (1961).
31. J. H. Piddington, *J. Geophys. Res.* **65**, 93 (1960).
32. L. A. Frank, *ibid.* **70**, 1593 (1965).
33. L. J. Cahill, *IGY Bull.* **79**, 231 (1964).
34. N. F. Ness, *J. Geophys. Res.* **70**, 2989 (1965).
35. J. H. Piddington, *Planetary Space Sci.* **13**, 363 (1965).
36. A. J. Dessler, *J. Geophys. Res.* **69**, 3913 (1964); ——— and R. D. Juday, *Planetary Space Sci.* **13**, 63 (1965).
37. W. I. Axford, H. E. Petschek, G. L. Siscoe, *J. Geophys. Res.* **70**, 1231 (1965).
38. K. W. Behannon and N. F. Ness, Goddard Space Flight Center preprint X-612-65-417 (1965).
39. I. A. McDiarmid and J. R. Burrows, *J. Geophys. Res.* **70**, 3031 (1965).
40. B. J. O'Brien, *Science* **148**, 449 (1965).
41. E. N. Parker, *Phys. Fluids* **1**, 171 (1958).
42. N. F. Ness and D. J. Williams, *J. Geophys. Res.* **71**, 322 (1966).
43. J. A. Van Allen, *ibid.* **70**, 4731 (1965).
44. E. J. Smith, L. Davis, Jr., P. J. Coleman, C. P. Sonett, *ibid.* **70**, 1571 (1965).
45. E. J. Smith, L. Davis, P. J. Coleman, D. E. Jones, *Science* **149**, 1241 (1965).
46. R. Hide and P. H. Roberts, in *Physics and Chemistry of the Earth*, L. H. Aherns *et al.*, Eds. (Pergamon, London, 1961), vol. 4, p. 27.
47. W. V. R. Malkus, *J. Geophys. Res.* **68**, 2871 (1963).
48. A. Cox, R. R. Doell, G. B. Dalrymple, *Science* **144**, 1537 (1964).

Physics in the Last Twenty Years

Emilio Segrè

Between 1895 and 1925, advances in physics probably came at a faster pace than in any comparable period since its beginning in modern form at the end of the 16th century.

Not only were entirely new phenomena, such as radioactivity, discovered, but also the very intellectual basis of physics was revolutionized by relativity and quantum theory. I would like to mention a few of the main conquests of these three startling decades in order to better evaluate more recent developments.

The 19th century closed with the discovery of the electron, x-rays, and

radioactivity. The 20th century opened with the hypothesis of the quanta of light, one of the strangest and most revolutionary ideas ever introduced in science. At that time classical physics had reached the peak of its perfection; according to some of its most illustrious students, the end of physics was perhaps in sight. Just at that time, ironically, a conservative perfectionist, to whom revolution was abhorrent, Max Planck, found himself compelled, in order to explain black-body radiation, to introduce a hypothesis that contradicted almost everything that was known in physics at the time. His

singular position is best illustrated by the fact—almost unique, as far as I know—that he had no precursors or rivals thinking along similar lines.

Einstein, who followed 5 years later with the special theory of relativity, radically changed our concepts of space and time, but he was far from alone in his line of thought.

The two great theoretical ideas, quantum theory and relativity—especially the first—were then applied to a marvelous supply of experimental facts which were discovered in the first decades of this century. The photoelectric effect, Rutherford's model of the atom, the Franck-Hertz experiment, the Stern-Gerlach experiment, the Compton effect, and the experimental discovery of de Broglie waves are some of the steps in this amazing progression.

The crowning achievement of this period was the development of a consistent form of quantum mechanics and the nearly complete understanding of the structure of the atom.

The author is professor of physics at the University of California, Berkeley. This article is adapted from an after-dinner address presented 27 December 1965 at the Berkeley meeting of the AAAS.